

Interfacial Layering in the Electric Double Layer of Ionic Liquids

J. Pedro de Souza,¹ Zachary A. H. Goodwin,^{2,3} Michael McEldrew^{1b},¹ Alexei A. Kornyshev^{1b,4,3} and Martin Z. Bazant^{1,5}

¹Department of Chemical Engineering, Massachusetts Institute of Technology, Cambridge, Massachusetts 02139, USA

²Department of Physics, CDT Theory and Simulation of Materials, Imperial College of London, South Kensington Campus, London SW7 2AZ, United Kingdom

³Thomas Young Centre for Theory and Simulation of Materials, Imperial College London, South Kensington Campus, London SW7 2AZ, United Kingdom

⁴Department of Chemistry, Imperial College of London, Molecular Science Research Hub, White City Campus, London W12 0BZ, United Kingdom

⁵Department of Mathematics, Massachusetts Institute of Technology, Cambridge, Massachusetts 02139, USA



(Received 15 May 2020; accepted 24 July 2020; published 8 September 2020)

Ions in ionic liquids and concentrated electrolytes reside in a crowded, strongly interacting environment, leading to the formation of discrete layers of charges at interfaces and spin-glass structure in the bulk. Here, we propose a simple theory that captures the coupling between steric and electrostatic forces in ionic liquids. The theory predicts the formation of discrete layers of charge at charged interfaces. Further from the interface, or at low polarization of the electrode, the model outputs slowly decaying oscillations in the charge density with a wavelength of a single ion diameter, as shown by analysis of the gradient expansion. The gradient expansion suggests a new structure for partial differential equations describing the electrostatic potential at charged interfaces. We find quantitative agreement between the theory and molecular simulations in the differential capacitance and concentration profiles.

DOI: 10.1103/PhysRevLett.125.116001

Introduction.—The spatial organization of ions in concentrated electrolytes leads to strong density and charge oscillations in the electric double layer (EDL) at charged interfaces [1–3]. When the concentration is beyond the dilute limit of the established Poisson-Boltzmann (PB) theory, one must account for correlation and packing effects, particularly as the Debye length approaches the size of a single ion [4]. Methods to correct the PB equations include the hypernetted-chain equation [5–10], mean-spherical approximation [11,12], density functional theory [13–21], and dressed-ion theory [22,23]. While many methods can accurately predict EDL profiles, they often lack the simplicity and physical transparency of the PB theory which they seek to correct [4].

More recently, with the rediscovery of room temperature ionic liquids (RTILs) [24,25] and their applications to energy storage devices [1,26], the task of understanding the interfacial structure in concentrated electrolytes has surged [27]. Describing the EDL of RTILs is particularly difficult because of the competition between strong steric and electrostatic forces [1], as illustrated in Fig. 1, and the fact that the expected Debye screening length is unphysically smaller than the diameter of an ion. In fact, the coupling of density and charge has been described as the ground state for a spin-glass Hamiltonian for ionic nearest neighbors (given their positions) [28], which is extremely difficult to describe with continuum equations. The interplay between ion position and charge order gives rise to the well-known

crossover from the overscreening regime (where decaying oscillations of charge density occur) to the crowding regime (where dense layers of countercharge accumulate first at the interface) [29–32].

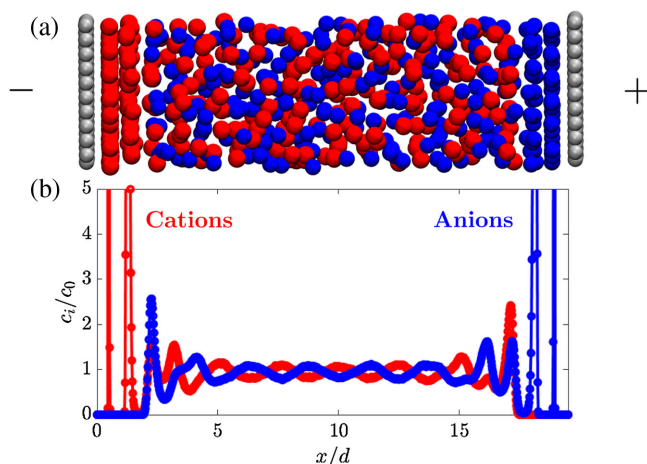


FIG. 1. (a) Illustration of a concentrated, crowded electrolyte forming structured double layers at high surface charge density. The cations are red, the anions are blue, and the surface atoms are shown in gray, with negative charge on the left surface and positive charge on the right surface. (b) Corresponding concentration profile for a model room temperature ionic liquid of equally sized, oppositely charged hard spheres ($c_0 = 5$ M, $d = 0.5$ nm, $\epsilon_r = 10$, $q_s = 120 \mu\text{C}/\text{cm}^2$, $T = 300$ K; for notations see text).

Perhaps one of the most popular descriptions of the overscreening versus crowding problem [29,30] in RTILs is the Bazant-Storey-Kornyshev (BSK) theory [31]. There, a higher order gradient term in electrostatic potential was proposed, in addition to the commonly used lattice-gas excluded-volume excess chemical potential [33,34]. The BSK theory has been shown also to describe well electrostatic correlations in dilute electrolytes and counterion only systems [35,36]. In the concentrated limit of RTILs, however, the BSK theory has some notable limitations: The screening is always short-ranged; the period of the oscillation is not necessarily the size of an ion, and the number and extent of oscillations is significantly underestimated. More recent work has suggested that the overscreening structure is a similar concept to the finite size [37] and orientation of ionic aggregates [38] near charged interfaces.

In this Letter, we propose a free-energy functional to describe the coupling between steric and electrostatic forces, and, therefore, capture the “spin-glass” nature of charge-mass correlations in RTILs. The theory predicts discrete layering, extended overscreening with a longer screening length than the size of an ion with an oscillation period of one ion diameter, and quantitative agreement with simulated differential capacitance. Our free-energy functional is a new hybrid approach using the weighted density approximation to describe the finite size of ions in both their electrostatic and steric interactions. Without fitting parameters, the theory has predictive capabilities, and it has a similar simplicity to the other modified-Poisson-Boltzmann approaches. While we explore the equilibrium properties at interfaces, the presented formulation could be extended to RTILs out of equilibrium, phase field crystal models, or systems including a structured solvent.

Theory.—We modify the electrostatic and hard sphere packing free energies by representing them in terms of weighted densities of local concentrations, similar to weighted-density approximations including fundamental measure theory [39–41]. We rationalize these choices by treating the ions as hard, conducting, charged spheres of finite size, each one a source of pseudopotential:

$$G_i(r) = \begin{cases} \frac{z_i e}{4\pi\epsilon r} & r \geq R \\ \phi_0 & r < R, \end{cases} \quad (1)$$

where ϕ_0 is a constant within a given ion, ϵ is the permittivity surrounding the ion (assumed constant in this work as an average effective background value), $z_i e$ is the charge of the ion, R its radius, and r is the distance from the center of an ion. The physical basis for the Ashcroft pseudopotential character [42] of the Green’s function is that the electrostatic potential within a finite-sized ion is effectively overwhelmed by the hard sphere potential within the ion. Therefore, the electrostatic potential is an

undefined constant within the sphere and can decay as a $1/r$ potential only beyond the ionic radius. The linear integro-differential equation corresponding to this Green’s function is

$$\begin{aligned} \epsilon \nabla^2 \phi &= -\bar{\rho}_e(\mathbf{r}) = - \int d\mathbf{r}' \rho_e(\mathbf{r}') w_s(\mathbf{r} - \mathbf{r}'), \\ w_s(\mathbf{r} - \mathbf{r}') &= \frac{1}{4\pi R^2} \delta(R - |\mathbf{r} - \mathbf{r}'|), \end{aligned} \quad (2)$$

which is the key modified mean-field Poisson equation in our work. Here ϕ is the electrostatic potential, $\rho_e = \sum_i z_i e c_i$ is the charge density of ionic centers, c_i is the number density of the centers of species i , $\bar{\rho}_e$ is the weighted charge density (calculated for the smeared charge of an ion over its surface), and w_s is the weighting function. Integrating contributions of the smeared charges results in the “actual” charge density which resides in the Poisson equation. While our weight function for the charge density resembles the choice of charge form factor in Ref. [37] for ionic screening in the bulk, we construct a mean-field equation that gives the ionic density at a flat interface at high surface charge density.

From the above modified Poisson equation, the electrostatic free-energy density becomes

$$\mathcal{F}^{\text{el}}[\bar{\rho}_e, \phi] = \int d\mathbf{r} \left\{ -\frac{\epsilon}{2} (\nabla\phi)^2 + \bar{\rho}_e \phi \right\}. \quad (3)$$

The chemical part of the free energy contains an ideal entropic contribution: $\mathcal{F}^{\text{id}}[\{c_i(\mathbf{r})\}] = \sum_i k_B T \int d\mathbf{r} c_i(\mathbf{r}) \times \{\ln[\Lambda^3 c_i(\mathbf{r})] - 1\}$, where $k_B T$ is thermal energy and Λ is the thermal de Broglie wavelength [39]. There is also an excess contribution from crowding of the finite-sized ions. The Carnahan-Starling equation of state accurately describes the properties of hard sphere liquids. Here, we adapt it and assume that the local excess free energy depends on volumetrically weighted densities, similar to fundamental measure theory [39,40],

$$\mathcal{F}^{\text{ex}}[\bar{c}_i(\mathbf{r})] = \frac{k_B T}{v} \int d\mathbf{r} \left[\frac{1}{1 - \bar{\rho}} - 3\bar{\rho} + \frac{1}{(1 - \bar{\rho})^2} \right], \quad (4)$$

where $\bar{\rho} = \sum_i v \bar{c}_i$ is the weighted volumetric filling fraction and $v = 4\pi R^3/3$ the volume of an ion. The weighted densities are defined by

$$\begin{aligned} \bar{c}_i(\mathbf{r}) &= \int d\mathbf{r}' c_i(\mathbf{r}') w_v(\mathbf{r} - \mathbf{r}'), \\ w_v(\mathbf{r} - \mathbf{r}') &= \frac{1}{v} \Theta(R - |\mathbf{r} - \mathbf{r}'|), \end{aligned} \quad (5)$$

where the scalar valued weighting function has units of inverse volume, and the function Θ represents a Heaviside step function. Therefore, the densities with which the

mean-field electrostatic interaction or hard sphere interaction occurs are computed with a quantized volume of one ion. Physically, the free energy is infinite as the volumetric-weighted filling fraction goes to one [43]. For the purposes of this study, the electrostatic charge density will be homogenized on a surface of an ionic sphere, whereas the volumetric packing fraction will be homogenized over a volume of an ionic sphere.

Minimizing the free-energy functional, we arrive at a modified PB equation, Eq. (2), where the distribution of ion (center) densities is determined by

$$c_i = c_{i,0} \exp(-z_i \beta e \bar{\phi} - \beta \bar{\mu}_i^{\text{ex}} + \beta \mu_{i,\text{bulk}}^{\text{ex}}), \quad (6)$$

with β as the inverse thermal energy, $\bar{\phi} = \phi * w_s$ and $\bar{\mu}_i^{\text{ex}} = \mu_i^{\text{ex}} * w_v$ (with $*$ denoting convolution), and excess chemical potential defined as $\beta \mu_i^{\text{ex}} = (8\bar{p} - 9\bar{p}^2 + 3\bar{p}^3)/(1 - \bar{p})^3$ [44].

Results and discussion.—We solve the above coupled integro-differential equations (2) and (6) at a flat electrode, with surface charge density q_s at $x = 0$. In this case, the standard boundary condition for the potential is applied, $\hat{\mathbf{n}} \cdot \epsilon \nabla \phi|_s = -q_s$. The local ionic densities (of centers) c_i and charge density (of ionic centers) ρ_e are assumed to be zero within one radius from the surface, from $x = 0$ to $x = R$, due to hard sphere exclusion. We solve for the area averaged density, and we therefore reduce all equations to be dependent on one coordinate, x . Numerically, we discretize the equations using a simple finite difference approach, similar to how the standard PB equations could be solved. More details on the numerics are provided in the Supplemental Material (SM) [47].

For further intuition, we analyze a simple gradient expansion of the weighting functions that turns them into operators: $w_j = 1 + \ell_j^2 \nabla^2$, where ℓ_j is given by $\ell_s = d/\sqrt{24}$ for w_s and $\ell_v = d/\sqrt{40}$ for w_v , as derived in the SM [47]. The corresponding differential form of the free-energy density is given by

$$\mathcal{F}^{\text{el}}[\bar{\rho}_e, \bar{\phi}] = \int d\mathbf{r} \left\{ -\frac{\epsilon}{2} (\nabla \bar{\phi})^2 + \bar{\rho}_e \bar{\phi} - \ell_s^2 \nabla \bar{\rho}_e \cdot \nabla \bar{\phi} \right\}. \quad (7)$$

The leading order term in the expansion corresponds to a dipole density interacting with an electric field, interpretable as ionic pairs of effective volumetric dipole moment $\ell_s^2 \nabla \bar{\rho}_e$, an effective polarization vector formed by gradients in the local charge density $\bar{\rho}_e$ [38]. Note that since the order of the differential form of Eq. (2) increases, we need an additional boundary condition. We assume this to be $\mathbf{n} \cdot \nabla \bar{\rho}_e|_s = 0$ in order to satisfy electro-neutrality in the differential equation, namely that $\int d\mathbf{r} \bar{\rho}_e(\mathbf{r}) = -\int d\mathbf{r} q_s(\mathbf{r}_s)$.

The above gradient expansion does not reproduce the profile at the initial contact of the ionic liquid with the surface. In particular, the differential form cannot capture the discontinuous contact point at $x = R$, and so the

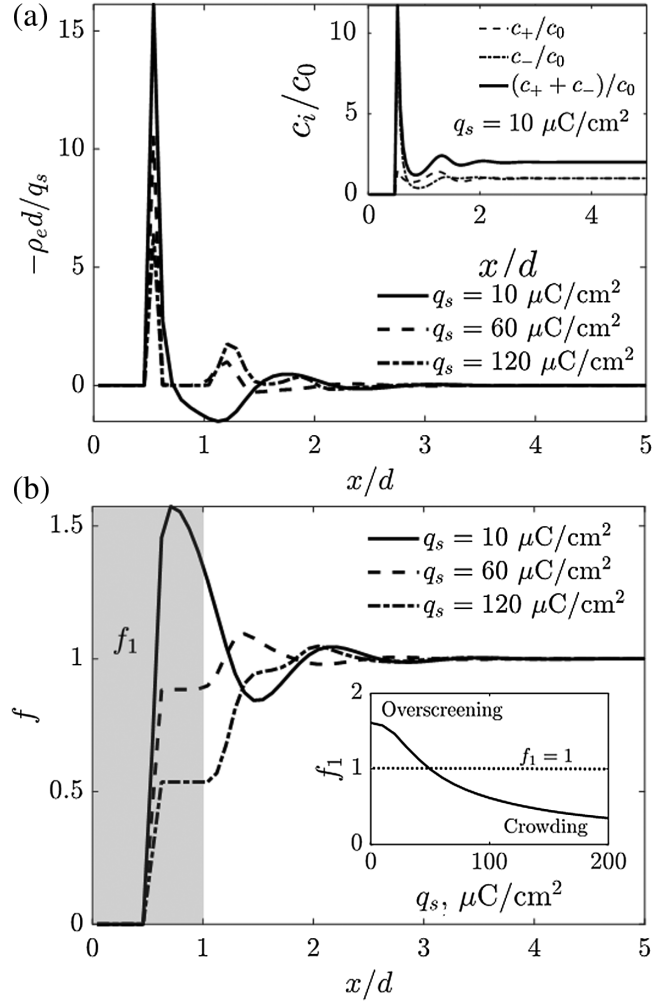


FIG. 2. Layering of ions in a concentrated electrolyte or ionic liquid. (a) The overscreening “signature”: the charge density of ions near a positively charged electrode scaled to the surface charge density on the electrode. The inset shows the concentration profile for each ion at $q_s = 10 \mu\text{C}/\text{cm}^2$, with oscillations in both the sum of concentrations and in the difference in concentrations. (b) The normalized cumulative charge density as a function of the distance from the interface, with inset showing the extent of screening in the first layer of charge f_1 , as explained in the text. Overscreening occurs when the net charge in the first layer is larger than the charge on the electrode.

solutions are shifted by one ionic radius. Even so, the gradient expansion is valid farther from the surface and is useful for deriving analytical approximations for the theory. Furthermore, the differential form may be easier to apply to problems in diverse applications such as electrokinetics [53], colloidal interactions [36], or electrochemical storage [54,55] than the full integro-differential theory [48]. As an example, we will first analyze the gradient expansion of the continuum theory in terms of its limiting linear response behavior, which asymptotically matches the behavior of the full integral equation far from the interface. Further comparisons are included in the SM [47].

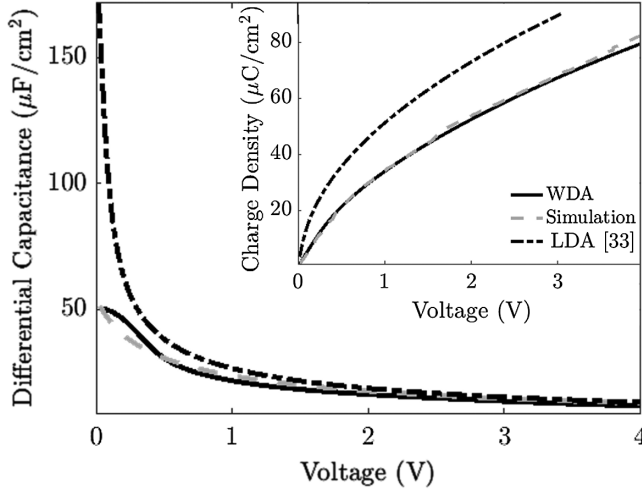


FIG. 3. Differential capacitance of the EDL as a function of the applied voltage, for the weighted density approximation (WDA) in Eq. (2), simulations, and the local density approximation (LDA) formula [33], given in the SM [47]. Inset: The charge density in the double layer as a function of the applied voltage. The parameters are identical to Fig. 2.

In linear response, the equation for the potential is

$$\lambda_D^2 \nabla^2 \phi - (1 + \ell_s^2 \nabla^2)^2 \phi = 0, \quad (8)$$

where λ_D is the Debye length. While the equation is fourth order, similar to the linearized BSK equation, it has different decaying modes due to an additional second order term. The eigenvalues of the above differential equation, denoted by the inverse decay length $\kappa_s = 1/\lambda_s$, have the form:

$$\kappa_s \lambda_D = \frac{1 \pm \sqrt{1 - 4(\ell_s/\lambda_D)^2}}{2(\ell_s/\lambda_D)^2}. \quad (9)$$

Note that the form of Eq. (8) bears some resemblance to the Swift-Hohenberg equation [56], commonly used to describe pattern formation and other phase-field crystal models [57]; here electrostatics and finite size drive the pattern formation. When $\ell_s/\lambda_D > 1/2$, oscillations appear in the solution, and in the limit of $\ell_s/\lambda_D \gg 1/2$, the screening length takes the form $\kappa_s \lambda_D = \lambda_D^2/\ell_s^2 \pm i\lambda_D/\ell_s$. At high concentration (small λ_D), the ions will therefore form charge density layers on the scale of the ionic size, with period of $1.28d$, similar to the result from simulations. In strongly correlated regimes, the real part of the screening length will scale as $\ln[\text{Re}(\lambda_s/\lambda_D)] = 2 \ln(d/\lambda_D) + \text{const}$, increasing with concentration. This result is qualitatively in agreement with surface force experiments [58,59], but they find a scaling factor 3 rather than 2. They also measure monotonic decay, and not decaying oscillations in the overscreening tail as predicted by the theory. Note that the mass density oscillations also have a characteristic decay length, but it is decoupled from the electrostatic potential at

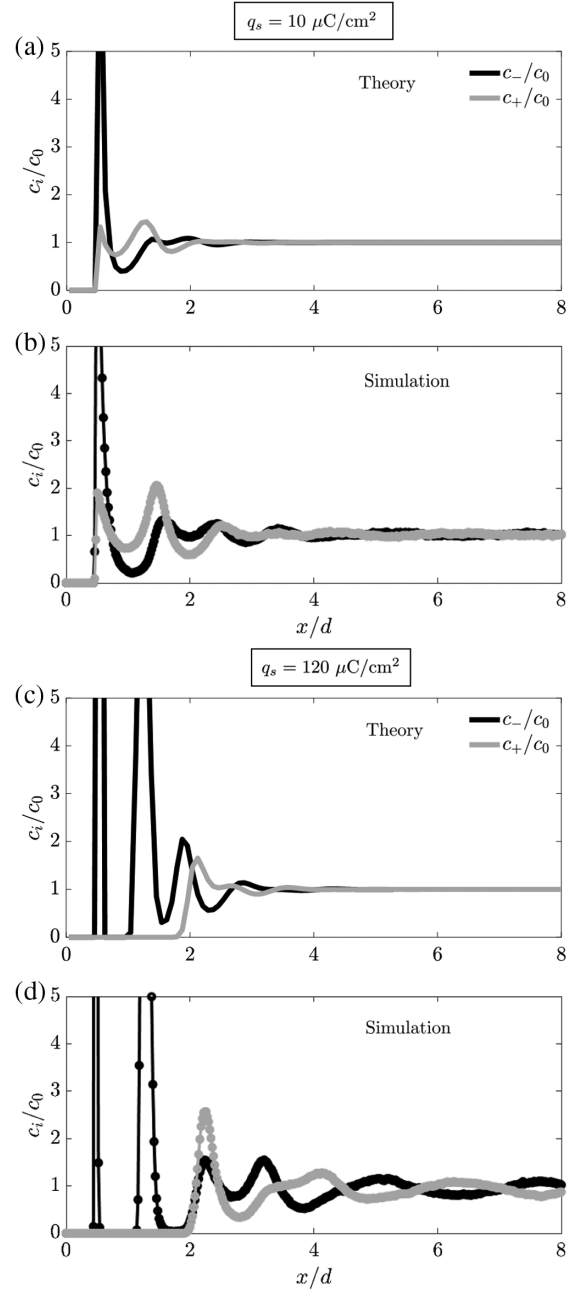


FIG. 4. Comparison of theory (a),(c) and simulation (b),(d) concentration profiles for two different charge densities: $q_s = 10 \mu\text{C}/\text{cm}^2$ and $q_s = 120 \mu\text{C}/\text{cm}^2$. The electrolyte has the same parameters as in Figs. 2 and 3 (Very large, exaggerated values of surface charge of $120 \mu\text{C}/\text{cm}^2$ are chosen for revealing the onset of crowding in the layers closest to the interface).

linear response for ions of the same size, as discussed in the SM [47]. The discrepancy in exponents may be due to the symmetric size of ions in the analysis here, which limits the coupling.

Next, we compute the ion concentration and density profiles as a function of charge density for some model parameters ($c_0 = 5 \text{ M}$, $d = 0.5 \text{ nm}$, $\epsilon_r = 10$, $T = 300 \text{ K}$), shown in Fig. 2. Note the parameters shown here are

meant to be representative of RTILs, but the simplifying assumptions of similarly sized spherical cations and anions prevent a direct comparison with experimental results for asymmetric ionic liquids of complicated shape [60]. We also present the cumulative screening charge, defined as $f(x) = -\int_0^x \rho_e(x') dx' / q_s$. At low surface charge density, the first layer of charge has about 57% more counter charge than the surface charge. Subsequent layers of alternating charge are formed. At low surface charge density, the ion concentrations themselves are affected by overall structuring of the fluid ($c_+ + c_-$) due to packing at the interface. At higher charge density, the inhibitive force of packing at the interface decreases the extent of overscreening in the first layer f_1 . Eventually, as the charge density exceeds the total amount of charge that can be stored in a single layer of ions, a secondary layer is formed. When this occurs, the extent of overscreening becomes determined by the renormalized charge on the interface. The chosen simulation parameters are in the strongly oscillating regime $\ell_s / \lambda_D \approx 2.1$, meaning that the far range screening tail has approximate wavelength of one ionic diameter and long decay length.

It is instructive to compare the predictions of the theory to MD simulations of a Lennard-Jones electrolyte with the same parameters. The differential capacitance, $C = |dq_s / d\phi_0|$, is evaluated in Fig. 3 as a function of the potential drop across the double layer, ϕ_0 . Compared to simulations, the weighted density theory captures the low capacitance at zero charge and further decrease of capacitance at large voltages. The theory presented here agrees much better with simulations compared to the local density approximation formula [33,61]; the improvements in the crowding regime, at large voltages, are due to use of the weighted Carnahan-Starling approximation rather than the simple local density approximation formula, both obeying, however, the $V^{-1/2}$ limiting law [33,48]. In Fig. 4, the layering structure is compared between theory and simulation for low and high charge densities. The theory is able to qualitatively match the structuring in the simulations, with charge density oscillations and eventually layers of the same charge at high charge density. Even so, the wavelength in the charge density oscillations are off by about a factor of 1.3. Such a discrepancy could be captured by changing the form of w_s to extend beyond the size of the ionic radius, but modifications to w_s are not considered in this work [62].

The developed continuum theory captures the key points in the interplay between overscreening and crowding in EDL of ionic liquids, including (1) decaying charge density profiles near the electrode and the overscreening effect as a consequence of molecular layering, (2) the onset of crowding through the shift of the overscreening to a third, and then subsequently further layers, and (3) the emergence of the long-range screening tail in ultraconcentrated ionic systems [63].

All authors acknowledge the support from the MIT-Imperial College Seed Fund. J. P. d. S acknowledges support from the Center for Enhanced Nanofluidic Transport, an Energy Frontier Research Center funded by the U.S. Department of Energy, Office of Science, Basic Energy Sciences under Award No. DE-SC0019112 (supporting simulations), and from the National Science Foundation Graduate Research Fellowship under Grant No. 1122374 (supporting theory development). M. M. was supported by the Amar G. Bose Research Grant. Z. A. H. G. was supported through a studentship in the Centre for Doctoral Training on Theory and Simulation of Materials at Imperial College London funded by the EPSRC (EP/L015579/1) and from the Thomas Young Centre under Grant No. TYC-101. A. A. K. acknowledges also The Leverhulme Trust (Grant No. RPG2016-223).

-
- [1] M. V. Fedorov and A. A. Kornyshev, *Chem. Rev.* **114**, 2978 (2014).
 - [2] M. Z. Bazant, M. S. Kilic, B. D. Storey, and A. Ajdari, *Adv. Colloid Interface Sci.* **152**, 48 (2009).
 - [3] J. G. Kirkwood, *Chem. Rev.* **19**, 275 (1936).
 - [4] L. M. Varela, M. Garcia, and V. Mosquera, *Phys. Rep.* **382**, 1 (2003).
 - [5] G. Patey, *J. Chem. Phys.* **72**, 5763 (1980).
 - [6] M. Lozada-Cassou, R. Saavedra-Barrera, and D. Henderson, *J. Chem. Phys.* **77**, 5150 (1982).
 - [7] R. Kjellander, T. Åkesson, B. Jönsson, and S. Marcelja, *J. Chem. Phys.* **97**, 1424 (1992).
 - [8] P. Attard, *Phys. Rev. E* **48**, 3604 (1993).
 - [9] R. Kjellander and D. J. Mitchell, *Chem. Phys. Lett.* **200**, 76 (1992).
 - [10] R. Kjellander, *J. Chem. Phys.* **148**, 193701 (2018).
 - [11] R. J. F. L. de Carvalho and R. Evans, *Mol. Phys.* **83**, 619 (1994).
 - [12] B. Rotenberg, O. Bernard, and J.-P. Hansen, *J. Phys. Condens. Matter* **30**, 054005 (2018).
 - [13] J. Lischner and T. A. Arias, *Phys. Rev. Lett.* **101**, 216401 (2008).
 - [14] K. Ma, J. Forsman, and C. E. Woodward, *J. Chem. Phys.* **142**, 174704 (2015).
 - [15] J. Reszko-Zygmunt, S. Sokołowski, D. Henderson, and D. Boda, *J. Chem. Phys.* **122**, 084504 (2005).
 - [16] L. B. Bhuiyan, S. Lamperski, J. Wu, and D. Henderson, *J. Phys. Chem. B* **116**, 10364 (2012).
 - [17] N. Gavish, D. Elad, and A. Yochelis, *J. Phys. Chem. Lett.* **9**, 36 (2018).
 - [18] J. Wu, T. Jiang, D.-e. Jiang, Z. Jin, and D. Henderson, *Soft Matter* **7**, 11222 (2011).
 - [19] D. Henderson, S. Lamperski, Z. Jin, and J. Wu, *J. Phys. Chem. B* **115**, 12911 (2011).
 - [20] K. Ma, C. Lian, C. E. Woodward, and B. Qin, *Chem. Phys. Lett.* **739**, 137001 (2020).
 - [21] A. Ciach, *J. Mol. Liq.* **270**, 138 (2018).
 - [22] R. Kjellander and D. J. Mitchell, *J. Chem. Phys.* **101**, 603 (1994).

- [23] M. Kanduč, A. Naji, J. Forsman, and R. Podgornik, *J. Chem. Phys.* **132**, 124701 (2010).
- [24] T. Welton, *Chem. Rev.* **99**, 2071 (1999).
- [25] J. P. Hallet and T. Welton, *Chem. Rev.* **111**, 3508 (2011).
- [26] S. Kondrat and A. A. Kornyshev, *Nanoscale Horiz.* **1**, 45 (2016).
- [27] S. Perkin, *Phys. Chem. Chem. Phys.* **14**, 5052 (2012).
- [28] A. Levy, M. McEldrew, and M. Z. Bazant, *Phys. Rev. Mater.* **3**, 055606 (2019).
- [29] M. V. Fedorov and A. A. Kornyshev, *Electrochim. Acta* **53**, 6835 (2008).
- [30] M. V. Fedorov, N. Georgi, and A. A. Kornyshev, *Electrochem. Comm.* **12**, 296 (2010).
- [31] M. Z. Bazant, B. D. Storey, and A. A. Kornyshev, *Phys. Rev. Lett.* **106**, 046102 (2011).
- [32] K. Kirchner, T. Kirchner, V. Ivaništšev, and M. V. Fedorov, *Electrochim. Acta* **110**, 762 (2013).
- [33] A. A. Kornyshev, *J. Phys. Chem. B* **111**, 5545 (2007).
- [34] M. S. Kilic, M. Z. Bazant, and A. Ajdari, *Phys. Rev. E* **75**, 021502 (2007).
- [35] J. P. de Souza and M. Z. Bazant, *J. Phys. Chem. C* **124**, 11414 (2020).
- [36] R. P. Misra, J. P. de Souza, D. Blankschtein, and M. Z. Bazant, *Langmuir* **35**, 11550 (2019).
- [37] R. M. Adar, S. A. Safran, H. Diamant, and D. Andelman, *Phys. Rev. E* **100**, 042615 (2019).
- [38] Y. Avni, R. M. Adar, and D. Andelman, *Phys. Rev. E* **101**, 010601(R) (2020).
- [39] R. Roth, *J. Phys. Condens. Matter* **22**, 063102 (2010).
- [40] Y. Rosenfeld, *Phys. Rev. Lett.* **63**, 980 (1989).
- [41] P. Tarazona, *Phys. Rev. A* **31**, 2672 (1985).
- [42] N. Ashcroft, *Phys. Lett.* **23**, 48 (1966).
- [43] The weighted density is necessary to describe the formation of discrete layers of charge at high surface charge density, which cannot be captured by local-density approximations.
- [44] A continuum theory of this kind does not require distinguishing “free,” “paired,” or “clustered” ions [45,46]. The ionic associations are reflected in oscillating charge density distributions.
- [45] M. McEldrew, Z. A. H. Goodwin, S. Bi, M. Z. Bazant, and A. A. Kornyshev, *J. Chem. Phys.* **152**, 234506 (2020).
- [46] G. Feng, M. Chen, S. Bi, Z. A. H. Goodwin, E. B. Postnikov, N. Brilliantov, M. Urbakh, and A. A. Kornyshev, *Phys. Rev. X*, **9**, 021024 (2019).
- [47] See Supplemental Material at <http://link.aps.org/supplemental/10.1103/PhysRevLett.125.116001> for numerical details, simulations details, and derivations of differential form of the theory, referencing Refs. [39,40,48–52].
- [48] M. Z. Bazant, M. S. Kilic, B. D. Storey, and A. Ajdari, *Adv. Colloid Interface Sci.* **152**, 48 (2009).
- [49] S. Plimpton and B. Hendrickson, *J. Comput. Phys.* **117**, 1 (1995).
- [50] L. Martínez, R. Andrade, E. G. Birgin, and J. M. Martínez, *J. Comput. Chem.* **30**, 2157 (2009).
- [51] A. Padua, *fftool: A tool to build force field input files for molecular dynamics* (2015), <https://github.com/agiliopadua/fftool>.
- [52] W. Humphrey, A. Dalke, K. Schulten, *J. Mol. Graphics* **14**, 33 (1996).
- [53] B. D. Storey and M. Z. Bazant, *Phys. Rev. E* **86**, 056303 (2012).
- [54] H. Zhao, *Phys. Rev. E* **84**, 051504 (2011).
- [55] M. McEldrew, Z. A. Goodwin, A. A. Kornyshev, and M. Z. Bazant, *J. Phys. Chem. Lett.* **9**, 5840 (2018).
- [56] J. Swift and P. C. Hohenberg, *Phys. Rev. A* **15**, 319 (1977).
- [57] K. R. Elder and M. Grant, *Phys. Rev. E* **70**, 051605 (2004).
- [58] A. A. Lee, C. Perez-Martinez, A. M. Smith, and S. Perkin, *Faraday Discuss.* **199**, 239 (2017).
- [59] A. M. Smith, A. A. Lee, and S. Perkin, *J. Phys. Chem. Lett.* **7**, 2157 (2016).
- [60] The symmetric size limits the possible parameter space due to maximal packing constraints, leading to a high differential capacitance at zero charge for both the theory and the simulation relative to experiments on real RTILs.
- [61] Z. A. H. Goodwin, G. Feng, and A. A. Kornyshev, *Electrochim. Acta* **225**, 190 (2017).
- [62] A different form of w_s implies different physical assumptions for the Green’s function in Eq. (1).
- [63] The integral theory also performs better than the BSK theory [31] in terms of describing the layered structure at the interface.